ACS Catalysis

Research Article

Cite This: ACS Catal. 2019, 9, 1026−1032

pubs.acs.org/acscatalysis

Realizing and Recognizing Syngas-to-Olefins Reaction via a Dual-Bed Catalyst

Youming Ni,[†,‡] Yong Liu,[†,‡] Zhiyang Chen,[†,‡,§] Miao Yang,[†,‡] Hongchao Liu,[†,‡] Yanli He,[†,‡] Yi Fu,[†,‡,§] Wenliang Zhu,*[,†,‡] and Zhongmin Liu*[,†,‡]

[†]National Engineering Laboratory for Methanol to Olefins, Dalian Institute of Chemical Physics, Chinese Academy of Sciences, Dalian 116023, China

[‡]Dalian National Laboratory for Clean Energy, Dalian Institute of Chemical Physics, Chinese Academy of Sciences, Dalian 116023, China

[§]University of Chinese Academy of Sciences, Beijing 100049, China

Supporting Information

ABSTRACT: Nowadays, a considerable progress in the syngas-to-olefins (STO) reaction has been made by physically mixed oxide-zeolite catalysts; however, contradictions concerning the reaction mechanism still exist. Although complete separation of the mixed catalysts should help to understand the STO reaction, it can result in lower CO conversion and selectivity of light olefins. Here, we report a stable and selective dual-bed STO catalyst $ZnAlO_x$/SAPO-34, which contains a SAPO-34 molecular sieve packed below $ZnAlO_x$ oxide. C_{2-4} olefins in hydrocarbons can reach 77.0% with only 33.1% CO_2 selectivity at 663 K. No significant deactivation is observed during a 100 h test. $ZnAlO_x$ itself can be used as a catalyst for the syngas-to-dimethyl ether (STD) reaction. Because the dual-bed catalyst presents similar reaction results and "hydrocarbon pool" intermediates to the mixed one, the STO reaction over a mixed catalyst can be understood as the combination of STD and MTO reactions regardless of catalytic behaviors and mechanisms.

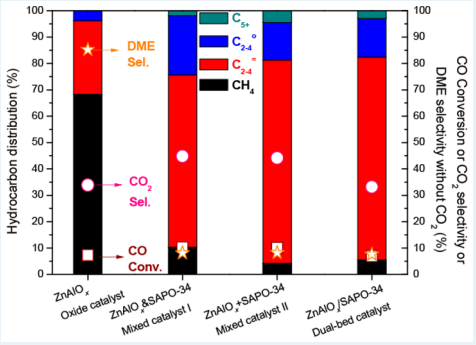

KEYWORDS: *heterogeneous catalysis, syngas-to-olefins, dual-bed catalyst, $ZnAlO_x$, SAPO-34*

INTRODUCTION

In recent years, syngas (CO and H_2) conversion captures more and more attention because of the following considerations: syngas can be derived from various nonpetroleum energy resources, such as coal, natural gas, biomass, and organic waste, and so on;[1] additionally, multitudinous clear fuels and bulk chemicals can be synthesized from syngas.[2−8]

Lower olefins are important basic chemicals which currently primarily come from petroleum by catalytic cracking. In order to reduce the dependence on oil resource, many works have been focused on producing lower olefins via Fischer−Tropsch synthesis.[9] However, the selectivity of C_{2-4} olefins and paraffins does not exceed 58% because of the restriction of Anderson−Schulz−Flory distribution.[10,11] C_{2-4} olefins could reach about 61% over cobalt carbide nanoprisms,[12] but higher utilization efficiency of syngas is still worth pursuing. Earlier, Minderhoud et al. reported that oxide-zeolite mixed catalysts could realize selective conversion of syngas to gasoline. However, high selectivity to light olefins has not been achieved by these mixed catalysts for a long period of time.[13] Recently, a pioneering work by Bao et al. reported that 80% C_{2-4} olefins could be achieved over a physically mixed bifunctional catalyst composed by $ZnCrO_x$ oxide and SAPO molecular sieve.[14] Simultaneously, Wang et al. reported that $ZnZrO_x$ mixed with SAPO-34 could also reach high C_{2-4} olefins selectivity in syngas conversion.[15] Later, even 73% ethylene has been obtained by Bao et al. over $ZnCrO_x$-MOR.[16] Interestingly enough, they have been holding different views on the active intermediates to olefins. Bao et al. proved that highly selective light olefins were more possibly derived from ketene (CH_2CO) intermediate generated over $ZnCrO_x$ rather than methanol or dimethyl ether (DME),[14,16] whereas Wang et al. considered that methanol and DME were major intermediates in their catalyst system.[8,15] Actually, syngas-to-olefins (STO) reaction over mixed oxide-zeolite catalyst is very complex. Judging from all of the STO products, at least four reactions are involved, which are methanol synthesis, methanol dehydration to DME, water−gas-shift (WGSR), and methanol (DME)-to-olefins (MTO). In addition, combined with the former three reactions, syngas-to-DME (STD) reaction can be achieved. If MTO reaction really takes place, long-term studies from our and other groups indicate that "hydrocarbon pool" intermediates could not be ignored.[17−24] Moreover, Brønsted acids of the zeolites can catalyze carbonylation and hydro-

Received: November 29, 2018
Revised: December 18, 2018
Published: December 21, 2018

DOI: 10.1021/acscatal.8b04794
ACS Catal. 2019, 9, 1026−1032

genation reactions, which would influence the product distribution.[25−29] Separation of the mixed oxide-zeolite catalyst, that is, dual-bed mode with zeolite downstream from oxide, should help to understand STO reaction; however, many facts tell us that it can result in lower CO conversion and light olefin selectivity with higher CH_4 selectivity.[14,15] Moreover, compared with a mixed catalyst, a dual-bed catalyst would have some advantages in reaction heat withdrawal and catalyst regeneration. Nowadays, developing an effective dual-bed STO catalyst remains challenging.

More recently, we have found that a nanoscaled spinel structural $ZnAlO_x$ oxide could catalyze CO_2 hydrogenation to dimethyl ether (DME) and methanol, and they were progressively converted into aromatics after being mixed with H-ZSM-5 zeolite.[30] Almost at the same time, Wang et al. reported that spinel $ZnAl_2O_4$ could also transform syngas into DME and methanol, and 65% ethylene was achieved over the mixed $ZnAl_2O_4$-MOR catalyst.[31] Up to now, successful application of $ZnAlO_x$ oxide into dual-bed STO catalyst has not been reported.

Here, we report a stable and selective dual-bed STO catalyst which contains SAPO-34 molecular sieve packed below $ZnAlO_x$ oxide. C_{2-4} olefins in the hydrocarbons can reach 77.0% with only 33.1% CO_2 selectivity at 663 K. No significant deactivation is observed during a 100 h reaction test. $ZnAlO_x$ itself is an excellent STD catalyst. STO reaction over mixed catalyst can be understood as the combination of STD and MTO reactions.

EXPERIMENTAL SECTION

Catalyst Preparation. $ZnAlO_x$ oxide catalyst was prepared by a typical coprecipitation method, which was reported in our recent study.[30] Briefly, 59.5 g of $Zn(NO_3)_26H_2O$ and 75.0 g of $Al(NO_3)_39H_2O$ were dissolved in 150 mL of deionized water. Then, 23.5 g of $(NH_4)_2CO_3$ was dissolved in 150 mL of deionized water. The two solutions were simultaneously added into one beaker with constant pH of 7.1−7.3 at 343 K under continuous stirring. The resultant precipitate was aged for 3 h at the same temperature. After it was filtered and thoroughly washed by deionized water, the obtained product was dried at 373 K overnight and then calcined in air at 773 K for 4 h. Al_2O_3 or n-ZnO was prepared by a precipitation method, which is similar to the procedures for preparing $ZnAlO_x$ except for not introducing $Zn(NO_3)_26H_2O$ or $Al(NO_3)_3$, respectively. Oxide m-ZnO was made by calcination of $Zn(NO_3)_26H_2O$ at 773 K for 4 h.

SAPO-34 molecular sieve (BET surface area = 324.2 $m^2\ g^{-1}$; Si/(Si+P+Al) molar ratio= 0.07) was supplied from 1202 Group in Dalian Institute of Chemical Physics (DICP). A dual-bed catalyst named $ZnAlO_x$/SAPO-34 contained $ZnAlO_x$ oxide in the upper bed and SAPO-34 in the lower bed. The two beds were completely separated by quartz wool. A physically mixed catalyst named $ZnAlO_x$+SAPO-34 was prepared by physically mixing the granules (0.4−0.8 mm) of two components. The granules in $ZnAlO_x$/SAPO-34 or $ZnAlO_x$+SAPO-34 were obtained by pressing under 40 MPa. Another physically mixed catalyst named $ZnAlO_x$&SAPO-34 was made by two-component grinding in an agate mortar for 4 min, and then they were pressed under 40 MPa and granulated into the required size in the range of 0.4−0.8 mm. The weight ratio of oxides and zeolites for the three catalysts above was 1:1. The physically mixed oxides called m-ZnO&Al_2O_3 or n-ZnO&Al_2O_3 were made by two-component grinding in an agate mortar for 4 min, and then they were pressed under 40 MPa and granulated into the required size in the range of 0.4−0.8 mm. In order to reach the same Zn content as $ZnAlO_x$, the weight ratio of m-ZnO (or n-ZnO) and Al_2O_3 was 1.1:1.

H-ZSM-5 zeolite (Si/Al = 96.6) and Si−H-ZSM-5 zeolite (Si/Al= 105.8) are the same as those in our recent work.[30] Si−H-ZSM-5 was prepared by TEOS modifying H-ZSM-5 for three times.

Catalytic Tests. Catalytic reaction experiments were carried out in a fixed-bed stainless steel reactor (8 mm inner diameter). All products were kept in gas phase and analyzed online by two tandem gas chromatographs. One is Agilent 7890A GC equipped with a HP-PLOT/Q capillary column connected to FID detector and a TDX-1 column connected to TCD detector. The other one is Agilent 7890B GC equipped with an HP-AL/S capillary column connected to FID detector and a TDX-1 column connected to TCD detector. CH_4 was used as a reference bridge between TCD and FID. Ar was used as an inner standard. Hydrocarbon distribution was based on carbon atoms number. CO conversion, CO_2 selectivity, and hydrocarbons (C_nH_m), MeOH, and DME selectivity excluding CO_2 were calculated with the following equations.

$$\text{CO conversion} = (CO_{in} - CO_{out})/(CO_{in}) \times 100\%$$

CO_{in}: moles of CO at the inlet;

CO_{out}: moles of CO at the outlet; (1)

$$CO_2 \text{ selectivity} = CO_{2out}/(CO_{in} - CO_{out}) \times 100\%$$

CO_{2out}: moles of CO_2 at the outlet; (2)

$$C_nH_m \text{ selectivity} = N_{C_nH_m}/(\text{all the carbon atoms of products in FID}) \times 100\%$$

$$\text{MeOH selectivity} = N_{MeOH}/(\text{all the carbon atoms of products in FID}) \times 100\%$$

$$\text{DME selectivity} = N_{DME}/(\text{all the carbon atoms of products in FID}) \times 100\%$$

$N_{C_nH_m}$: the number of carbon atoms for C_nH_m;

N_{MeOH}: the number of carbon atoms for MeOH;

N_{DME}: the number of carbon atoms for DME. (3)

An Agilent 6890N GC equipped with a HP-FFAP capillary column connected to FID detector was employed to supply a detailed analysis for aromatics such as ethylbenzene, *p*-xylene, *m*-xylene, and *o*-xylene.[30]

Characterization of Catalysts. The XRD tests were performed on a PANalytical X'Pert PRO X-ray diffractometer with Cu Kα radiation. Element analysis was carried out on a Philips Magix-601 X-ray fluorescence (XRF) spectrometer. SEM measurements were performed on an SU8020 scanning electron microscopy. The BET surface areas were tested by N_2 adsorption at 77 K on a Micromeritics ASAP 2020 system. In situ DRIFTS studies were performed on a Bruker Tensor 27 instrument with a MCT detector. $ZnAlO_x$ powder was pressed into a diffuse reflectance infrared cell with ZnSe window. First, $ZnAlO_x$ was treated by 30 mL min^{-1} H_2/Ar (H_2/Ar = 3/7) mixture at 0.1 MPa and 593 K for 0.5 h, and the background spectrum was recorded. Then, 30 mL min^{-1} mixed gas (H_2/CO = 1/1) was introduced and the in situ DRIFT spectra

DOI: 10.1021/acscatal.8b04794
ACS Catal. 2019, 9, 1026−1032

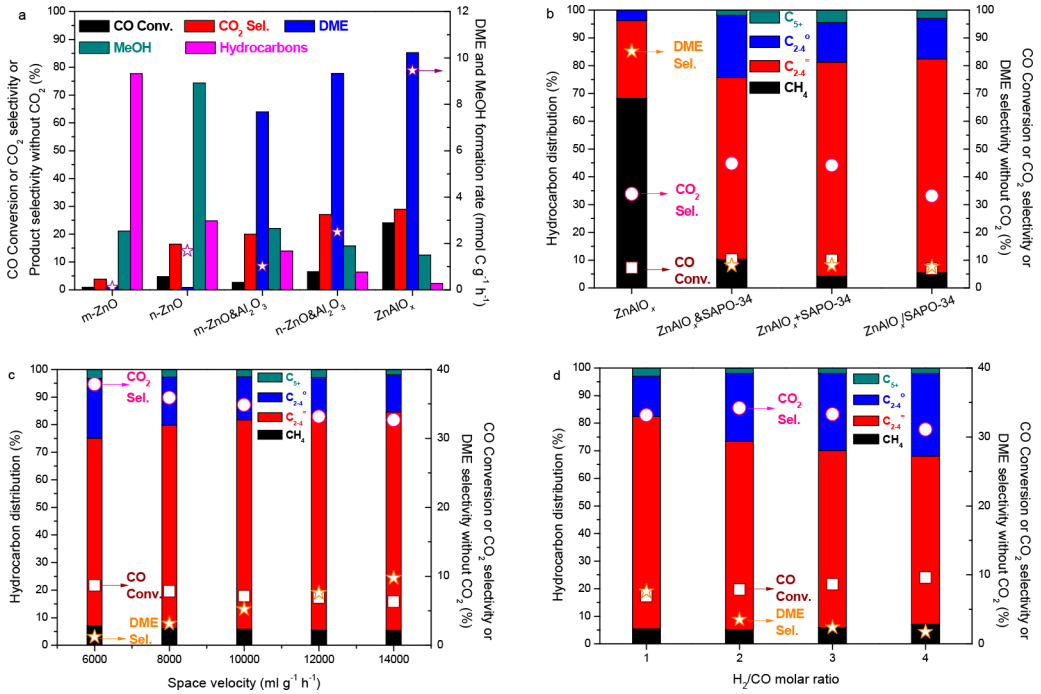

Figure 1. Catalytic results for syngas conversion over various catalysts. (a) STD performances. $H_2/CO/Ar$ = 2/1/0.1, Space velocity (based on all reactants at STP in this paper) = 4000 mL g^{-1} h^{-1}, 633 K, 4.0 MPa. (b) STO performances over dual-bed and mixed catalysts. $H_2/CO/Ar$= 1/1/0.1, Space velocity = 12 000 mL g^{-1} h^{-1} (or 24 000 mL g^{-1} h^{-1} for $ZnAlO_x$), 663 K, 4.0 MPa. (c) The effect of space velocity over dual-bed $ZnAlO_x$/SAPO-34. $H_2/CO/Ar$ = 1/1/0.1, 663 K, 4.0 MPa. (d) The effect of H_2/CO ratio over dual-bed $ZnAlO_x$/SAPO-34. Space velocity = 12 000 mL g^{-1} h^{-1}, 663 K, 4.0 MPa. Note that C_{5+} includes hydrocarbons with no less than 5 carbons. $C_{2-4}^{=}$ and C_{2-4}° refer to C_{2-4} olefins and paraffins, respectively; m-ZnO&Al_2O_3, n-ZnO&Al_2O_3 and $ZnAlO_x$&SAPO-34 prepared by grinding; $ZnAlO_x$+SAPO-34 prepared by granules mixing; $ZnAlO_x$/SAPO-34 denoted as dual-bed catalyst.

obtained by collecting 32 scans at 4 cm^{-1} resolution were recorded under the same conditions. FTIR spectra after pyridine adsorption were collected on a Bruker Tensor 27 instrument with a resolution of 4 cm^{-1}. X-ray photoelectron spectroscopy (XPS) measurements were carried out on a Thermofisher ESCALAB 250Xi spectrometer. The organic materials retained in SAPO-34 after reactions were analyzed by M. Guisnet's method.[32] Spent SAPO-34 catalysts were dissolved in HF solution (20 wt %). After being neutralized with NaOH solution (5 wt %), the soluble organics were extracted by CH_2Cl_2 (containing 10 ppm of C_2Cl_6) and then analyzed by using a GC-MS instrument (Agilent 7890B) equipped with an HP-5 capillary column.

RESULTS AND DISCUSSION

Considering that syngas conversion should primarily take place on the oxide layer of the dual-bed catalyst, we first explored catalytic behaviors of $ZnAlO_x$. Five oxide catalysts containing Zn were compared under reaction conditions of H_2/CO = 2/1, space velocity (based on all reactants at STP in this paper) = 4000 mL g^{-1} h^{-1}, 4.0 MPa, and 633 K (Figure 1a). The m-ZnO prepared by calcination of $Zn(NO_3)_26H_2O$ shows a very low CO conversion (0.9%). Hydrocarbons are predominant products. Compared with m-ZnO, the n-ZnO made by precipitation obviously exhibits an improved activity with 4.7% CO conversion and 74.4% MeOH (excluding CO_2). When m-ZnO or n-ZnO is physically mixed with Al_2O_3 obtained by precipitation, the CO conversion is further increased and DME becomes the primary product. CO_2 which is formed by WGSR reaction is also increased after mixing Al_2O_3. DME selectivity (excluding CO_2) reaches up to 77.8% over n-ZnO&Al_2O_3 (physical mixture) along with 6.5% CO conversion and 15.8% MeOH selectivity. It is apparent that methanol dehydration and WGSR reactions can promote methanol synthesis. It is surprising to see that the $ZnAlO_x$ prepared by coprecipitation presents much better performance than n-ZnO&Al_2O_3. CO conversion over $ZnAlO_x$ runs up to 24.1% with 85.3% DME selectivity and 12.5% MeOH selectivity. CO_2 (28.9%) over $ZnAlO_x$ is approximate to that over n-ZnO&Al_2O_3. Furthermore, the DME and MeOH formation rate over $ZnAlO_x$ can achieve 9.5 mmol C g^{-1} h^{-1}, which is 3.8 times as high as n-ZnO&Al_2O_3. These results above suggest that the coprecipitated $ZnAlO_x$ should be not equivalent to the mixture of precipitated n-ZnO and Al_2O_3. Figure S1 shows that catalytic activity over $ZnAlO_x$ can reach to a maximum at 633 K. Figure S2 presents that the DME and MeOH formation rate over $ZnAlO_x$ is almost linearly increased with space velocity rising. Figure S3 indicates that increasing reaction pressure helps to promote CO conversion. Figure S4 suggests that low H_2/CO molar ratio favors the formation of DME.

We designed a dual-bed catalyst named $ZnAlO_x$/SAPO-34 which contained $ZnAlO_x$ in the upper bed and SAPO-34 molecular sieve in the lower bed. The two beds were completely separated by quartz wool. Surprisingly, $ZnAlO_x$/SAPO-34 exhibits an excellent STO performance (Figure 1b). 77.0% C_{2-4} olefins and 5.5% CH_4 in the hydrocarbons are achieved along with 6.9% CO conversion and only 33.1% CO_2 selectivity under reaction conditions of H_2/CO = 1/1, space velocity = 12 000 mL g^{-1} h^{-1}, 4.0 MPa, and 663 K. Propylene is predominant in the C_{2-4} olefins (Figure S5). $ZnAlO_x$ almost presents equivalent CO conversion and CO_2 selectivity to

DOI: 10.1021/acscatal.8b04794
ACS Catal. 2019, 9, 1026−1032

$ZnAlO_x$/SAPO-34, which indicates that CO hydrogenation and WGSR reactions substantially occurs on oxide layer. DME selectivity (excluding CO_2)) over $ZnAlO_x$/SAPO-34 is much less than $ZnAlO_x$, which means that the light olefins produced by dual-bed catalyst are primarily derived from DME conversion. Although $ZnAlO_x$+SAPO-34 which prepared by the granules of two components mixing shows 77.0% C_{2-4} olefins in hydrocarbons and even higher CO conversion (10.1%) than $ZnAlO_x$/SAPO-34, it also yields more CO_2 (44.1%). It suggests that, with regard to $ZnAlO_x$+SAPO-34, H_2O synthesized from DME conversion over SAPO-34 component can promote the formation of CO_2 over $ZnAlO_x$ component via WGSR reaction. By calculation, C_{2-4} olefins formation rate over $ZnAlO_x$+SAPO-34 (126.5 mg g^{-1} h^{-1}) is approximate to $ZnAlO_x$/SAPO-34 (111.7 mg g^{-1} h^{-1}). These results above suggest that STO reaction over mixed catalyst could be understood as the combination of STD and MTO reactions over dual-bed catalyst. Furthermore, the CO conversion and CO_2 selectivity over $ZnAlO_x$&SAPO-34 made by two components grinding in an agate mortar are approximate to those over $ZnAlO_x$+SAPO-34, but the former produces less C_{2-4} olefins. As the space velocity rising from 6000 to 14 000 mL g^{-1} h^{-1}, the C_{2-4} olefins in hydrocarbons are increased from 68.0% to 79.1% with the C_{2-4} paraffins accordingly decreasing (Figure 1c). Previous studies have proved that Brønsted acid of the zeolites can catalyze olefins hydrogenation to paraffins,[25,26] which could be the major challenge to develop a highly selective STO dual-bed catalyst. The result above demonstrates that olefins hydrogenation reaction can be substantially depressed by increasing space velocity. Figure 1d shows that lower H_2/CO ratio in the syngas feed leads to higher C_{2-4} olefins. Figure S6 suggests that raising reaction temperature can strengthen hydrogenation of C_{2-4} olefins to paraffins. Moreover, dual-bed $ZnCrO_x$/SAPO-34 shows a low CO conversion (~2%) with high CH_4 (~10%) in hydrocarbons (Figure S7), which is consistent to Bao's work.[14] As we know, $ZnCrO_x$ oxide is a conventional methanol synthesis catalyst. Previous calculation results indicated that high reaction temperature (above 600 K) was detrimental to methanol synthesis.[15]

The catalytic stability of the dual-bed $ZnAlO_x$/SAPO-34 catalyst has been investigated at 658 K. As shown in Figure 2a and Figure S8, a long induction period (about 20 h) can be observed. Induction period, which is believed to be related to the formation of "hydrocarbon pool" intermediates,[17−24] is transient in the conventional MTO reaction. These intermediates generally include unsaturated species such as aromatics.[17−24] Therefore, the existence of H_2 under high pressure should be disadvantage to produce them. C_{2-4} olefins in hydrocarbons reach to 78.3% at 20 h on stream then slightly decay to 76.6% after 100 h. CO conversion (7.4%) and CO_2 selectivity (32.8%) are almost unchanged. $ZnAlO_x$ itself delivers an excellent stability (Figure 2b). The CO conversion, DME or MeOH selectivity is kept at around 24%, 85% or 13% in a 100 h test at 633 K and H_2/CO = 2/1, respectively. In fact, STD reaction is also important and has been extensively studied these years.[33] A lot of research has focused on hybridized methanol synthesis (e.g., $CuZnAlO_x$) and solid acid dehydration catalysts (e.g., zeolites and γ-Al_2O_3).[33] Generally, Cu-based catalysts for methanol synthesis are stably operated below 523 K; however, dehydration catalysts start to exhibit an effective performance above this temperature. For this reason, in the most STD studies, the suitable reaction temperatures are

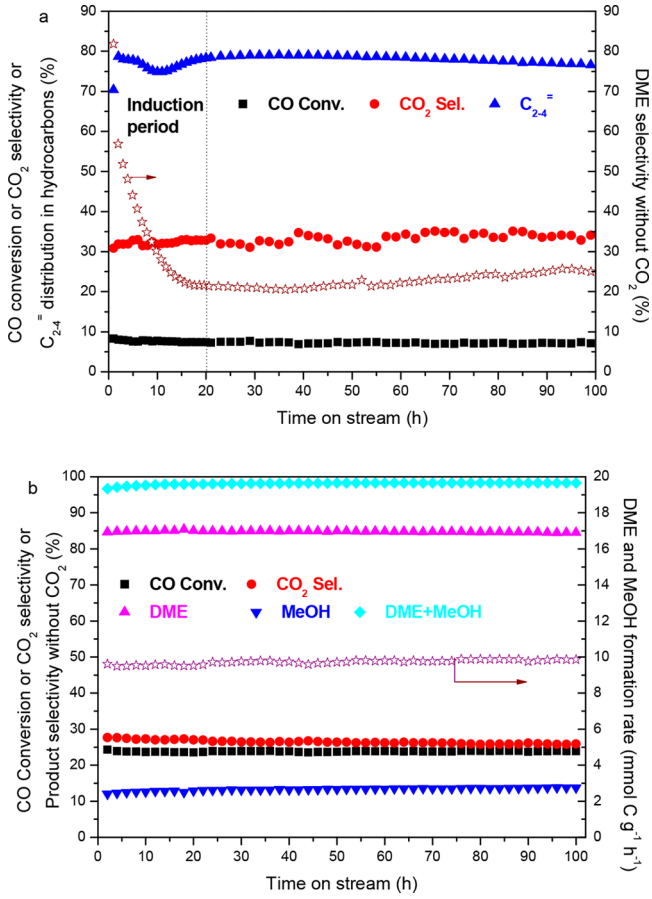

Figure 2. Stability tests for STO and STD reactions. (a) STO over dual-bed $ZnAlO_x$/SAPO-34. H_2/CO/Ar = 1/1/0.1, space velocity = 12 000 mL g^{-1} h^{-1}, 658 K, 4.0 MPa. (b) STD over $ZnAlO_x$. H_2/CO/Ar = 2/1/0.1, space velocity = 4000 mL g^{-1} h^{-1}, 4.0 MPa, 633 K.

focused on the range from 523 to 573 K, which results in a poor stability of the hybridized catalysts.[33] Compared with Cu-based hybridized catalysts, $ZnAlO_x$, which possesses good activity and stability, suggests a more promising application in producing DME from syngas.

Conversion of methanol with H_2 or CO cofeed over SAPO-34 was investigated to interpret the performance of the dual-bed $ZnAlO_x$/SAPO-34 catalyst. Compared with cofeeding H_2, cofeeding CO leads to higher initial methanol conversion, light olefins selectivity and deactivation rate (Figure 3). It means that the functions of H_2 and CO are very different on the lower SAPO-34 layer of the dual-bed catalyst. Recently, Bhan et al. found that the lifetime of SAPO-34 could be dramatically improved by high-pressure H_2 cofeed in MTO reaction without obviously decreasing light olefin selectivity (~85%).[34] By calculation, their space velocity is about 7.3 × 10^6 mL g^{-1} h^{-1} at 3.0 MPa. Therefore, lower light olefins produced from methanol cofed with H_2 in Figure 3 could be rationalized due to much lower space velocity (~10 000 mL g^{-1} h^{-1}). Unlike MeOH-H_2 as feed, MeOH-Ar as feed presents normal high methanol conversion and light olefin selectivity. Moreover, the deactivation rate for Ar cofeed is lower than that for CO cofeed.

Given that ZSM-5 zeolite is another typical MTO catalyst, we also explored the STO behaviors of dual-bed $ZnAlO_x$/H-ZSM-5 catalyst (Figure S9). Compared with $ZnAlO_x$/SAPO-34 under the same reaction conditions, $ZnAlO_x$/H-ZSM-5

DOI: 10.1021/acscatal.8b04794
ACS Catal. 2019, 9, 1026−1032

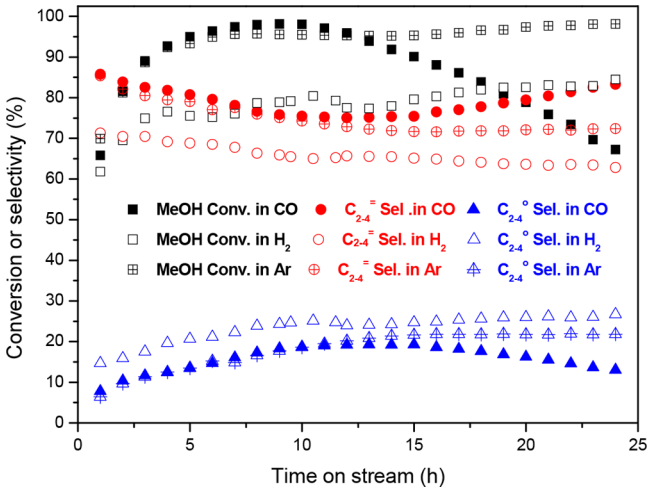

Figure 3. Methanol conversion with H_2, CO or Ar cofeed over SAPO-34. H_2 (CO or Ar)/MeOH molar ratio = 238/1, space velocity = 10 042 mL g^{-1} h^{-1}, 658 K, 4.0 MPa. DME is treated as reactant.

evidently exhibits lower olefins/paraffins ratio in C_{2-4} hydrocarbons (O/P ratio), which suggests that hydrogenation ability of H-ZSM-5 is stronger than SAPO-34. After modified by tetraethoxysilane (TEOS), the resultant dual-bed $ZnAlO_x$/Si−H-ZSM-5 shows a substantial improvement in O/P ratio. As recently reported,[30] TEOS modification led to a decline of acid amount, which accordingly helped with depressing hydrogenation. It is worth noting that other valuable hydrocarbons such as BTX and *p*-xylene are also increased and *p*-xylene in xylenes rises up to 60.1% over $ZnAlO_x$/Si−H-ZSM-5.

Soluble carbonaceous deposits in SAPO-34 layer of dual-bed $ZnAlO_x$/SAPO-34 catalyst after reaction were analyzed by GC-MS. Methylbenzenes (species of 1−8), methylnaphthalenes (species of 9−14), phenanthrene (species of 15), and pyrene (species of 16) are observed in Figure 4a. These aromatic species, especially methylbenzenes (species of 1−8), should act as "hydrocarbon pool" intermediates because the used $ZnAlO_x$/SAPO-34 is still active (7.1% CO conversion) and selective (74.1% C_{2-4} olefins). As shown in Figure 4b, organic materials retained in SAPO-34 component of the mixed $ZnAlO_x$+SAPO-34 after reaction are analogous to those in Figure 4a. Therefore, we consider that STO reaction over mixed catalyst is substantially the combination of STD and MTO reactions over dual-bed catalyst in mechanism. We also observed a lot of aromatic species in the SAPO-34 after MeOH−CO cofed, but their amount was very low after MeOH-H_2 cofed (Figure S11). It indicates that CO favors the formation of aromatic "hydrocarbon pool" intermediates, whereas H_2 intercepts their generation. Our recent work has proved that CO could promote aromatization via Koch carbonylation mechanism.[35] Bhan et al. has reported that H_2 could suppress the generation of polycyclic aromatics via interception of the formaldehyde-mediated alkylation reactions.[34] Therefore, the synergy of H_2 and CO is very important to STO reaction.

XRD patterns (Figure S12) show that the $ZnAlO_x$ oxide has a typical spinel structure assigned to $ZnAl_2O_4$ gahnite.[30] In contrast to $ZnAlO_x$, n-ZnO&Al_2O_3 presents reflection peaks of ZnO. Although the chemical elements composition of $ZnAlO_x$ is the same as n-ZnO&Al_2O_3, the activity of the former is much higher than the latter (Figure 1a), which indicates that the

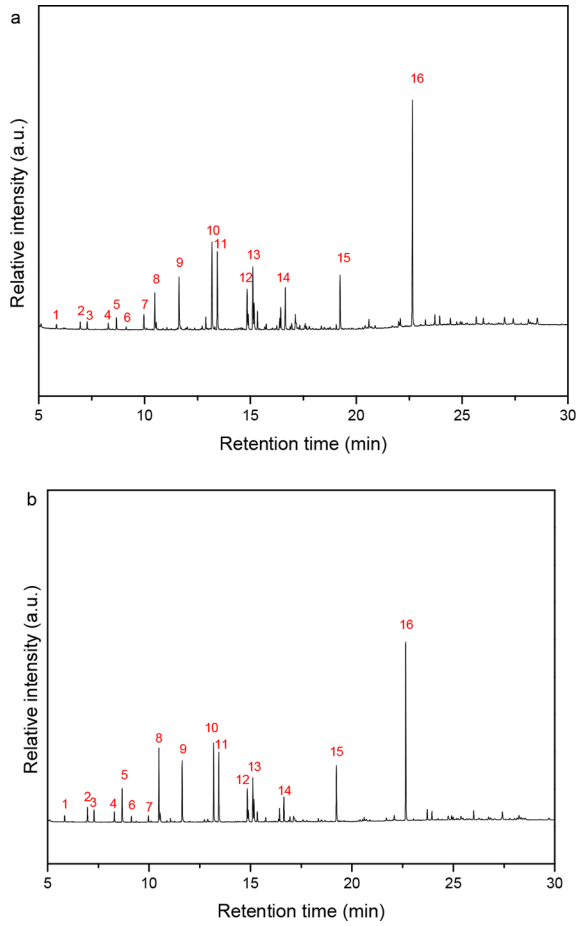

Figure 4. GC-MS chromatograms of the organic materials retained in SAPO-34 components of spent dual-bed $ZnAlO_x$/SAPO-34 (a) and spent physically mixed $ZnAlO_x$+SAPO-34 (b). The spent dual-bed $ZnAlO_x$/SAPO-34 was obtained after 163 h on stream under the same conditions in Figure 2a. The spent physically mixed $ZnAlO_x$+SAPO-34 was obtained after reaction in Figure S10. C_2Cl_6 is used as the internal standard. 1: toluene; 2 and 3: xylenes; 4, 5 and 6: trimethyl-benzenes; 7: C_2Cl_6; 8: tetramethyl-benzene; 9: naphthalene; 10 and 11: methyl-naphthalenes; 12 and 13: dimethyl-naphthalenes; 14: trimethyl-naphthalene; 15: phenanthrene; 16: pyrene.

spinel structure plays a significant role in syngas conversion. XRD patterns of SAPO-34 present typical CHA structure (Figure S13). SEM images (Figure S14) show that the particle size of n-ZnO (~100 nm) is much smaller than m-ZnO (~20 μm). Figure 1a shows that n-ZnO presents a higher syngas conversion than m-ZnO. It is believed that reducing the particle size of catalysts is propitious to improve the catalytic performance via exposing more inside active sites. $ZnAlO_x$ and Al_2O_3 exhibit porous structures made by tiny particles. As recently reported,[30] the particle size of $ZnAlO_x$ is less than 10 nm. SEM image (Figure S15) suggests that the particle size of SAPO-34 is about 5 μm. The band at 1450 cm^{-1} in the FTIR spectra after pyridine adsorption (Figure S16) demonstrates that $ZnAlO_x$ includes a lot of Lewis acid sites, which should be acted as catalysis center for methanol dehydration. X-ray photoelectron spectroscopy (XPS) measurements were carried out to explore the surface Zn species changes of $ZnAlO_x$ after in situ H_2 treatment at 633 K (Figure S17). Zn LMM Auger spectroscopy of fresh $ZnAlO_x$ presents a peak at 987.5 eV, which is assigned to Zn^{2+}.[36] After reduction, any substantial change in the peak position or shape cannot be observed.

DOI: 10.1021/acscatal.8b04794
ACS Catal. 2019, 9, 1026−1032

Because LMM Auger spectroscopy is more sensitive than other XPS signals to detect the oxidation state change of Zn,[37] it is very possible that in situ H_2 treatment at 633 K is not able to reduce Zn^{2+} of $ZnAlO_x$ to its metal phase. Therefore, we infer that Zn^{2+} of $ZnAlO_x$ may remain unchanged under the real reaction conditions. Zn 2p3/2 spectra of fresh $ZnAlO_x$ can be resolved into two peaks lying at 1022.1 and 1021.2 eV, which are associated with Zn^{2+} in Zn−O bonds and oxygen vacancies regions, respectively.[38] According to the calculation results in Table S1, H_2 treatment hardly influences the oxygen vacancies related to Zn species. Moreover, formate and methoxy species can be observed by in situ DRIFTS (Figure S18) of syngas conversion over $ZnAlO_x$.

According to the findings in this paper, we propose a mechanism for STO reaction over a dual-bed catalyst $ZnAlO_x$/SAPO-34. First, since HO-Zn can be readily generated by oxygen vacancies[38] and Al_2O_3 is inactive for syngas conversion, we deduce that the surface formate species should be H(CO)O−Zn, which is formed by HO-Zn reacted with CO. Because the primary product over n-ZnO is methanol, H(CO)O−Zn could be continuously hydrogenated to CH_3OH and HO-Zn. CH_3OH then spreads to Lewis acid sites ($^+$Al−O−Al-O^-) to obtain CH_3O−Al−O-Al−OH.[33] DME can be generated by the reaction: 2 CH_3O−Al−O-Al−OH = CH_3OCH_3 + H_2O + 2 ($^+$Al−O−Al-O^-). DME with unreacted syngas is then transmitted to SAPO-34. After producing enough "hydrocarbon pool" intermediates, light olefins are finally synthesized.

CONCLUSIONS

In conclusion, we have succeeded in designing a selective and stable dual-bed STO catalyst named $ZnAlO_x$/SAPO-34. C_{2-4} olefins in the hydrocarbons reach as high as 77.0% along with 6.9% CO conversion and only 33.1% CO_2 selectivity. No obvious deactivation is observed during a 100 h STO reaction test. $ZnAlO_x$ itself is an excellent STD catalyst. STO reaction over mixed oxide-zeolite catalyst can be understood as the combination of STD and MTO reactions regardless of catalytic results and mechanisms.

ASSOCIATED CONTENT

Supporting Information

The Supporting Information is available free of charge on the ACS Publications website at DOI: 10.1021/acscatal.8b04794.

Detailed catalytic results and characterization results (PDF)

AUTHOR INFORMATION

Corresponding Authors

*E-mail: liuzm@dicp.ac.cn.
*E-mail: wlzhu@dicp.ac.cn.

ORCID

Zhongmin Liu: 0000-0001-8439-2336

Notes

The authors declare no competing financial interest.

ACKNOWLEDGMENTS

We acknowledge the financial support from the National Natural Science Foundation of China (Grant No. 21606224). We thank Weichen Zhang for assistance in the experiments.

REFERENCES

(1) Torres Galvis, H. M.; de Jong, K. P. Catalysts for Production of Lower Olefins from Synthesis Gas: A Review. *ACS Catal.* **2013**, *3*, 2130−2149.
(2) Khodakov, A. Y.; Chu, W.; Fongarland, P. Advances in the Development of Novel Cobalt Fischer−Tropsch Catalysts for Synthesis of Long-Chain Hydrocarbons and Clean Fuels. *Chem. Rev.* **2007**, *107*, 1692−1744.
(3) Calderone, V. R.; Shiju, N. R.; Curulla-Ferre, D.; Chambrey, S.; Khodakov, A.; Rose, A.; Thiessen, J.; Jess, A.; Rothenberg, G. De novo Design of Nanostructured Iron-Cobalt Fischer−Tropsch Catalysts. *Angew. Chem., Int. Ed.* **2013**, *52*, 4397−4401.
(4) Cheng, K.; Zhou, W.; Kang, J.; He, S.; Shi, S.; Zhang, Q.; Pan, Y.; Wen, W.; Wang, Y. Bifunctional Catalysts for One-Step Conversion of Syngas into Aromatics with Excellent Selectivity and Stability. *Chem.* **2017**, *3*, 334−347.
(5) Zhao, B.; Zhai, P.; Wang, P.; Li, J.; Li, T.; Peng, M.; Zhao, M.; Hu, G.; Yang, Y.; Li, Y. W.; Zhang, Q.; Fan, W.; Ma, D. Direct Transformation of Syngas to Aromatics over Na-Zn-Fe_5C_2 and Hierarchical HZSM-5 Tandem Catalysts. *Chem.* **2017**, *3*, 323−333.
(6) Zhang, P.; Tan, L.; Yang, G.; Tsubaki, N. One-pass Selective Conversion of Syngas to Para-Xylene. *Chem. Sci.* **2017**, *8*, 7941−7946.
(7) Zhu, Y.; Pan, X.; Jiao, F.; Li, J.; Yang, J.; Ding, M.; Han, Y.; Liu, Z.; Bao, X. Role of Manganese Oxide in Syngas Conversion to Light Olefins. *ACS Catal.* **2017**, *7*, 2800−2804.
(8) Liu, X.; Zhou, W.; Yang, Y.; Cheng, K.; Kang, J.; Zhang, L.; Zhang, G.; Min, X.; Zhang, Q.; Wang, Y. Design of Efficient Bifunctional Catalysts for Direct Conversion of Syngas into Lower Olefins via Methanol/Dimethyl Ether Intermediates. *Chem. Sci.* **2018**, *9*, 4708−4718.
(9) Torres Galvis, H. M.; Bitter, J. H.; Khare, C. B.; Ruitenbeek, M.; Dugulan, A. I.; de Jong, K. P. Supported Iron Nanoparticles as Catalysts for Sustainable Production of Lower Olefins. *Science* **2012**, *335*, 835−838.
(10) Friedel, R. A.; Anderson, R. B. Composition of Synthetic Liquid Fuels. I. Product Distribution and Analysis of C_5-C_8 Paraffin Isomers from Cobalt Catalyst. *J. Am. Chem. Soc.* **1950**, *72*, 1212−1215.
(11) Puskas, I.; Hurlbut, R. S. Comments about the Causes of Deviations from the Anderson-Schulz−Flory Distribution of the Fischer−Tropsch Reaction Products. *Catal. Today* **2003**, *84*, 99−109.
(12) Zhong, L.; Yu, F.; An, Y.; Zhao, Y.; Sun, Y.; Li, Z.; Lin, T.; Lin, Y.; Qi, X.; Dai, Y.; Gu, L.; Hu, J.; Jin, S.; Shen, Q.; Wang, H. Cobalt Carbide Nanoprisms for Direct Production of Lower Olefins from Syngas. *Nature* **2016**, *538*, 84−87.
(13) Minderhoud, J. K.; Post, M. F. M. Preparation of Hydrocarbon Mixtures from Syngas. U.S. Patent 4507404, 1985.
(14) Jiao, F.; Li, J.; Pan, X.; Xiao, J.; Li, H.; Ma, H.; Wei, M.; Pan, Y.; Zhou, Z.; Li, M.; Miao, S.; Li, J.; Zhu, Y.; Xiao, D.; He, T.; Yang, J.; Qi, F.; Fu, Q.; Bao, X. Selective Conversion of Syngas to Light Olefins. *Science* **2016**, *351*, 1065−1068.
(15) Cheng, K.; Gu, B.; Liu, X.; Kang, J.; Zhang, Q.; Wang, Y. Direct and Highly Selective Conversion of Synthesis Gas into Lower Olefins: Design of a Bifunctional Catalyst Combining Methanol Synthesis and Carbon-Carbon Coupling. *Angew. Chem., Int. Ed.* **2016**, *55*, 4725−4728.
(16) Jiao, F.; Pan, X.; Gong, K.; Chen, Y.; Li, G.; Bao, X. Shape-Selective Zeolites Promote Ethylene Formation from Syngas via a Ketene Intermediate. *Angew. Chem., Int. Ed.* **2018**, *57*, 4692−4696.
(17) Haw, J. F.; Song, W.; Marcus, D. M.; Nicholas, J. B. The Mechanism of Methanol to Hydrocarbon Catalysis. *Acc. Chem. Res.* **2003**, *36*, 317−326.
(18) Mores, D.; Stavitski, E.; Kox, M. H.; Kornatowski, J.; Olsbye, U.; Weckhuysen, B. M. Space- and Time-Resolved In-situ Spectroscopy on the Coke Formation in Molecular Sieves: Methanol-to-Olefin Conversion over H-ZSM-5 and H-SAPO-34. *Chem. - Eur. J.* **2008**, *14*, 11320−11327.
(19) Li, J.; Wei, Y.; Chen, J.; Tian, P.; Su, X.; Xu, S.; Qi, Y.; Wang, Q.; Zhou, Y.; He, Y.; Liu, Z. Observation of Heptamethylbenzenium

DOI: 10.1021/acscatal.8b04794
ACS Catal. 2019, 9, 1026−1032

Cation over SAPO-Type Molecular Sieve DNL-6 under Real MTO Conversion Conditions. *J. Am. Chem. Soc.* **2012**, *134*, 836−839.
(20) Xu, S.; Zheng, A.; Wei, Y.; Chen, J.; Li, J.; Chu, Y.; Zhang, M.; Wang, Q.; Zhou, Y.; Wang, J.; Deng, F.; Liu, Z. Direct Observation of Cyclic Carbenium Ions and Their Role in the Catalytic Cycle of the Methanol-To-Olefin Reaction over Chabazite Zeolites. *Angew. Chem., Int. Ed.* **2013**, *52*, 11564−11568.
(21) Wei, Y.; Li, J.; Yuan, C.; Xu, S.; Zhou, Y.; Chen, J.; Wang, Q.; Zhang, Q.; Liu, Z. Generation of Diamondoid Hydrocarbons as Confined Compounds in SAPO-34 Catalyst in the Conversion of Methanol. *Chem. Commun.* **2012**, *48*, 3082−3084.
(22) Wu, X.; Xu, S.; Zhang, W.; Huang, J.; Li, J.; Yu, B.; Wei, Y.; Liu, Z. Direct Mechanism of the First Carbon-Carbon Bond Formation in the Methanol-To-Hydrocarbons Process. *Angew. Chem., Int. Ed.* **2017**, *56*, 9039−9043.
(23) Tian, P.; Wei, Y. X.; Ye, M.; Liu, Z. M. Methanol to olefins (MTO): From Fundamentals to Commercialization. *ACS Catal.* **2015**, *5*, 1922−1938.
(24) Dahl, I. M.; Kolboe, S. On the Reaction-Mechanism for Propene Formation in the MTO Reaction over SAPO-34. *Catal. Lett.* **1993**, *20*, 329−336.
(25) Senger, S.; Radom, L. Zeolites as Transition-Metal-Free Hydrogenation Catalysts: A Theoretical Mechanistic Study. *J. Am. Chem. Soc.* **2000**, *122*, 2613−2620.
(26) Kanai, J.; Martens, J. A.; Jacobs, P. A. On the Nature of the Active Sites for Ethylene Hydrogenation in Metal-Free Zeolites. *J. Catal.* **1992**, *133*, 527−543.
(27) Cheung, P.; Bhan, A.; Sunley, G. J.; Iglesia, E. Selective Carbonylation of Dimethyl Ether to Methyl Acetate Catalyzed by Acidic Zeolites. *Angew. Chem., Int. Ed.* **2006**, *45*, 1617−1620.
(28) Bhan, A.; Allian, A. D.; Sunley, G. J.; Law, D. J.; Iglesia, E. Specificity of Sites within Eight-Membered Ring Zeolite Channels for Carbonylation of Methyls to Acetyls. *J. Am. Chem. Soc.* **2007**, *129*, 4919−4924.
(29) Ni, Y. M.; Shi, L.; Liu, H. C.; Zhang, W. N.; Liu, Y.; Zhu, W. L.; Liu, Z. M. A Green Route for Methanol Carbonylation. *Catal. Sci. Technol.* **2017**, *7*, 4818−4822.
(30) Ni, Y.; Chen, Z.; Fu, Y.; Liu, Y.; Zhu, W.; Liu, Z. Selective Conversion of CO_2 and H_2 into Aromatics. *Nat. Commun.* **2018**, *9*, 3457.
(31) Zhou, W.; Kang, J.; Cheng, K.; He, S.; Shi, J.; Zhou, C.; Zhang, Q.; Chen, J.; Peng, L.; Chen, M.; Wang, Y. Direct Conversion of Syngas into Methyl Acetate, Ethanol, and Ethylene by Relay Catalysis via the Intermediate Dimethyl Ether. *Angew. Chem., Int. Ed.* **2018**, *57*, 12012−12016.
(32) Guisnet, M.; Magnoux, P. Coking and Deactivation of Zeolites: Influence of the Pore Structure. *Appl. Catal.* **1989**, *54*, 1−27.
(33) Saravanan, K.; Ham, H.; Tsubaki, N.; Bae, J. W. Recent Progress for Direct Synthesis of Dimethyl Ether from Syngas on the Heterogeneous Bifunctional Hybrid Catalysts. *Appl. Catal., B* **2017**, *217*, 494−522.
(34) Arora, S. S.; Nieskens, D. L. S.; Malek, A.; Bhan, A. Lifetime Improvement in Methanol-to-Olefins Catalysis over Chabazite Materials by High-Pressure H_2 Co-Feeds. *Nat. Catal.* **2018**, *1*, 666−672.
(35) Chen, Z.; Ni, Y.; Zhi, Y.; Wen, F.; Zhou, Z.; Wei, Y.; Zhu, W.; Liu, Z. Coupling of Methanol and Carbon Monoxide over H-ZSM-5 to Form Aromatics. *Angew. Chem., Int. Ed.* **2018**, *57*, 12549−12553.
(36) Kattel, S.; Ramirez, P. J.; Chen, J. G.; Rodriguez, J. A.; Liu, P. Response to Comment on "Active Sites for CO_2 Hydrogenation to Methanol on Cu/ZnO Catalysts. *Science* **2017**, *357* (6354), eaan8210.
(37) Nakamura, J.; Fujitani, T.; Kuld, S.; Helveg, S.; Chorkendorff, I.; Sehested, J. Comment on "Active sites for CO_2 Hydrogenation to Methanol on Cu/ZnO Catalysts. *Science* **2017**, *357* (6354), eaan8074.
(38) Yang, C.; Wang, J.; Fan, H. L.; Shangguan, J.; Mi, J.; Huo, C. Contributions of Tailored Oxygen Vacancies in ZnO/Al_2O_3 Composites to the Enhanced Ability for H_2S Removal at Room Temperature. *Fuel* **2018**, *215*, 695−703.

DOI: 10.1021/acscatal.8b04794
ACS Catal. 2019, 9, 1026−1032